A Diagnostic Approach in Alzheimer's Disease Using Three-Dimensional Stereotactic Surface Projections of Fluorine-18-FDG PET

Satoshi Minoshima, Kirk A. Frey, Robert A. Koeppe, Norman L. Foster and David E. Kuhl

Division of Nuclear Medicine, Department of Internal Medicine, and Departments of Neurology and Radiology, University of Michigan, Ann Arbor, Michigan

To improve the diagnostic performance of PET as an aid in evaluating patients suspected of having Alzheimer's disease, we developed a fully automated method which generates comprehensive image presentations and objective diagnostic indices. **Methods:** Fluorine-18-fluorodeoxyglucose PET image sets were collected from 37 patients with probable Alzheimer's disease (including questionable and mild dementia), 22 normal subjects and 5 patients with cerebrovascular disease. Following stereotactic anatomic standardization, metabolic activity on an individual's PET image set was extracted to a set of predefined surface pixels (three-dimensional stereotactic surface projection, 3D-SSP), which was used in the subsequent analysis. A normal database was created by averaging extracted datasets of the normal subjects. Patients' datasets were compared individually with the normal database by calculating a Z-score on a pixel-by-pixel basis and were displayed in 3D-SSP views for visual inspections. Diagnostic indices were then generated based on averaged Z-scores for the association cortices. **Results:** Patterns and severities of metabolic reduction in patients with probable Alzheimer's disease were seen in the standard 3D-SSP views of extracted raw data and statistical Z-scores. When discriminating patients with probable Alzheimer's disease from normal subjects, diagnostic indices of the parietal association cortex and unilaterally averaged parietal-temporal-frontal cortex showed sensitivities of 95% and 97%, respectively, with a specificity of 100%. Neither index yielded false-positive results for cerebrovascular disease. **Conclusion:** 3D-SSP enables quantitative data extraction and reliable localization of metabolic abnormalities by means of stereotactic coordinates. The proposed method is a promising approach for interpreting functional brain PET scans.

Key words: Alzheimer's disease; positron emission tomography; glucose metabolism; image interpretation; brain mapping

J Nucl Med 1995; 36:1238–1248

For more than a decade, PET has been used to investigate functional alteration of the brain in patients with Alzheimer's disease (*1–5*). Various researchers have demonstrated metabolic and blood flow reductions in the parietotemporal association cortex, widely recognized as a diagnostic pattern for Alzheimer's disease on functional brain images (*3–17*). The presence of such a diagnostic pattern facilitated the use of both PET and SPECT in clinical settings to evaluate patients with dementia. In the previous studies, however, subjective approaches were often used to diagnose Alzheimer's disease with functional images, such as visual pattern recognition and visually placed ROI analysis. A goal of this study is to develop an objective and accurate method of analysis to enhance the diagnostic performance of cerebral glucose metabolic PET studies in Alzheimer's disease.

An assumption required for discriminating Alzheimer's disease with PET is that regional cerebral glucose metabolism measured using [^{18}F]fluorodeoxyglucose (FDG) should show certain stereotypical features which are distinguishable from those of normal subjects and other pathological conditions. According to previous observations, we hypothesize that the following features observed on PET glucose metabolic images are patterns suggestive of Alzheimer's disease:

1. In Alzheimer's disease, glucose metabolism is most often affected in the parietotemporal association cortex (*3–17*).
2. The involvement is bilateral, although asymmetry in the degree of metabolic reduction is recognized (*4,9,10,15,18–20*).
3. Glucose metabolism in the frontal association cortex is reduced in certain cases, often in advanced disease (*8,10,13,16,21*).
4. The primary neocortical regions, such as sensorimotor and visual cortices, as well as subcortical structures, such as the thalamus, are relatively spared (*2,13,15,16*).

The proposed method is not aimed at simply exploring new discriminators but incorporating these known metabolic features of Alzheimer's disease into the algorithm and generating an objective index and image presentation. The

Received Jul. 18, 1994; accepted Jan. 25, 1995.

For correspondence or reprints contact: Satoshi Minoshima, MD, PhD, Division of Nuclear Medicine, Department of Internal Medicine, The University of Michigan Medical Center, B1-G412 University Hospital, 1500 E. Medical Center Dr., Ann Arbor, MI 48109-0028.

method proposed is also designed to satisfy these conditions:

1. To achieve objective and reproducible analyses, the method is automated fully.
2. Image processing and anatomic interpretation are performed in the standard bicommissural stereotactic system to facilitate accurate signal localization and cross-institutional comparisons.
3. The method is stable and insensitive to anatomic variations across subjects or groups.
4. The method does not require quantitative measurement of cerebral glucose metabolism, avoiding arterial blood sampling.
5. The processed data are displayed objectively for visual inspection by different observers.
6. The method is applicable in a routine clinical setting with acceptable computational time.

In this article, we present methods for image processing and presentation, examine characteristics of functional abnormalities in Alzheimer's disease compared with normal control subjects, describe diagnostic indices based on Z-scores and evaluate diagnostic accuracy using PET image sets from normal subjects and from patients with Alzheimer's or cerebrovascular disease.

MATERIALS AND METHODS

Patients and Subjects

The proposed methodology was evaluated in 37 patients with probable Alzheimer's disease using a database of 22 similar-aged normal controls. Additionally, image sets from five patients with cerebrovascular diseases were tested to assess the specificity of the diagnostic index. Distributions of age and sex were 64 ± 7.5 (mean and s.d.) and 7:15 (men:women) in normal controls, 68 ± 6.8 and 15:22 in Alzheimer's disease and 67 ± 11 and 3:2 in cerebrovascular disease, respectively. None of the volunteers had any prior history of neurological or psychiatric disorder or any major medical illness. Each normal volunteer had a routine neurological examination on the day of PET imaging. Diagnosis of probable Alzheimer's disease was based on National Institute of Neurological and Communicative Disorders and Stroke (NINCDS) and Alzheimer's Disease and Related Disorders Association (ADRDA) criteria (*29,30*). In patients with probable Alzheimer's disease, absence of focal cerebral abnormalities was confirmed by x-ray CT and/or MRI. Hachinski's Ischemic Scores (*31,32*) were less than four in all of the patients. Of the 37 patients with Alzheimer's disease, three patients were questionably demented (Clinical Demetia Rating (*33*), CDR = 0.5), 23 patients were mildly demented (CDR = 1), seven patients were moderately demented (CDR = 2), and four patients were severely demented (CDR = 3) at the time of the PET study. All subjects satisfied NINCDS-ADRDA dementia criteria on subsequent clinical follow-up over a year. Five patients with cerebrovascular disease underwent MRI, and the presence and locations of infarctions were confirmed by radiologists. This group includes two patients with large right middle cerebral artery territory infarcts (1 and 5 mo after onset), two patients with multiple cortical infarcts with dementia, and one patient with small cortical infarcts associated with subcortical lacunar infarcts.

Fluorine-18-2-fluoro-2-deoxy-D-glucose (FDG) PET image sets were acquired following intravenous administration of 10 mCi (370 MBq) [^{18}F]FDG using a Siemens ECAT 931/08-12 scanner (CTI Inc., Knoxville, TN), which collects 15 simultaneous slices with a slice separation of 6.75 mm. Tomographic images were reconstructed using a Shepp filter with cutoff frequency of 0.35 cycles/projection element. Attenuation correction was performed by a standard ellipse-fitting method. Reconstructed raw counts were converted linearly to quantitative glucose metabolic rates by a standard single scan method using an input function obtained from the radial artery (*34*). These image sets were analyzed in quantitative and nonquantitative (with normalization) fashions in the following validations.

Metabolic Abnormalities in Alzheimer's Disease

To confirm characteristics of metabolic abnormalities in Alzheimer's disease, regional metabolic activity was summarized in terms of quantitative cerebral glucose metabolic rate (CMRglc), normalized CMRglc to the thalamus, Z-score reduction and ΔZ-score. Regional CMRglc was determined on the cortical extraction data for parietal, temporal, frontal and occipital cortices specified by the same stereotactic grid coordinates used in the Z-score analysis. CMRglc of the primary sensorimotor cortex was measured from the location determined automatically by the above algorithm. Two sample t-tests (for CMRglc and normalized CMRglc) and Mann-Whitney U-tests (for Z-score reduction and ΔZ-score) with Bonferroni corrections were used to describe significance of differences between two groups on those measurements.

Patterns of Cortical Abnormalities in Alzheimer's Disease

To confirm patterns of regional metabolic abnormalities on each hemisphere in Alzheimer's disease, we categorized regional trends in cortical metabolic reduction based on ΔZ-scores. For example, if ΔZ-scores were larger in the parietal > temporal > frontal cortices, the hemispheric abnormality was categorized as P > T > F. The same analysis was performed in the normal group, and differences in patterns between normals and patients with Alzheimer's disease were assessed. When calculating ΔZ-score for normal controls, a jackknife-type procedure was used as described in the next section. Second, using the same analysis, symmetry in regional trends of metabolic abnormalities between two hemispheres was assessed for each subject. When the patterns of metabolic abnormalities were identical between two hemispheres, the subject was categorized as symmetrical. The same analysis was performed in the normal group, and the results were compared with those from the patient group. Chi-square tests were used for assessing differences between two groups.

Determination for Optimal Thresholds for ΔZ-score

A ΔZ-score threshold which was optimal for discriminating Alzheimer's disease from normal was determined based on sensitivity and specificity in the given datasets of normal and Alzheimer's disease. To calculate specificity, we used the following technique based on a jackknife-type procedure (*35*). First, normal reference data were calculated from 21 subjects excluding one subject. Z-score data of the excluded subject were then calculated in comparison to the normal reference data created from the rest of the normal controls. This procedure was repeated 22 times to generate individual Z-score data for each normal control. The rest of the analysis was the same as for Alzheimer's disease patients.

By changing the Z-score threshold, sensitivity and specificity in discriminating Alzheimer's disease were calculated and demonstrated using a form of receiver-operator-characteristics (ROC)

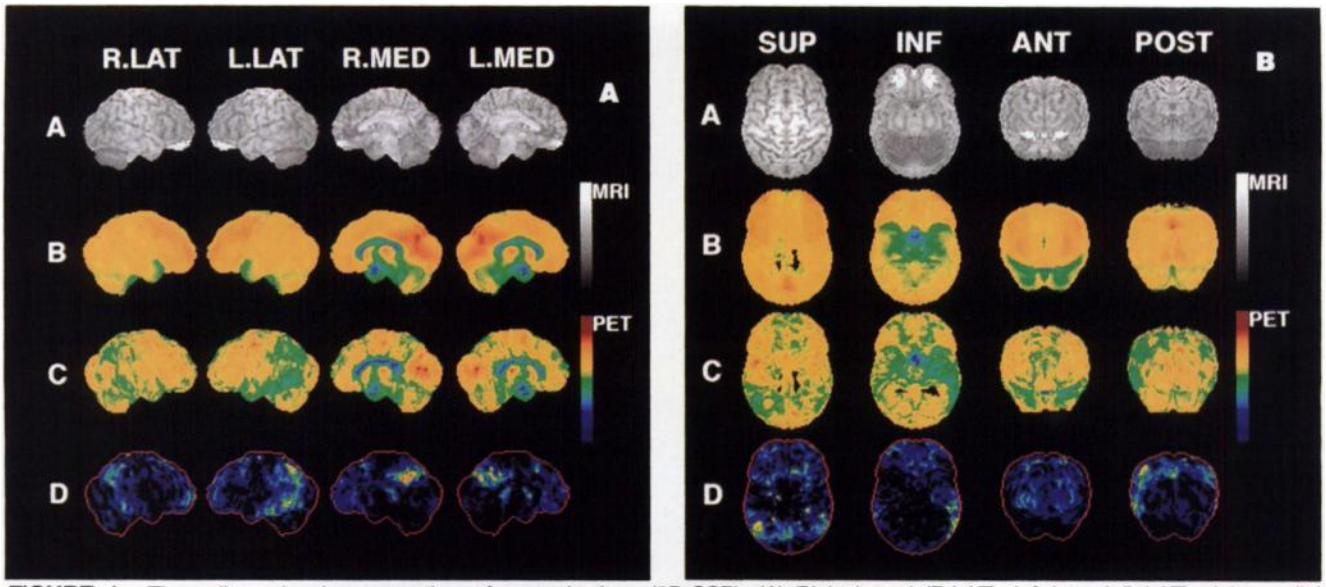

FIGURE 1. Three-dimensional stereotactic surface projections (3D-SSP). (A) Right lateral (R.LAT), left lateral (L.LAT), right medial (R.MED), and left medial (L.MED) views. (B) Superior (SUP), inferior (INF), anterior (ANT), and posterior (POST) views. Row A: Reference for surface anatomy of the brain revealed by MR imaging. Row B: 3D-SSP of a normal database representing mean pixel values averaged across 22 normal subjects on a pixel-by-pixel basis. Row C: 3D-SSP of CMRglc from a representative patient with Alzheimer's disease (70 year-old female, CDR = 1). Row D: 3D-SSP of statistical Z-scores representing areas of functional reduction in the patient in comparison with the normal database.

(*36*). The threshold was assessed independently for parietal, temporal, and frontal ΔZ-score indices, as well as for the unilaterally averaged parieto-temporo-frontal index. When evaluating parietal, temporal, and frontal indices, the same threshold was applied to both hemispheres. The diagnosis was based on the bilateral abnormalities (when each hemisphere was diagnosed independently as 'abnormal' based on the given threshold), as previously discussed.

Comparison with A/N Ratio

The ΔZ-score discrimination was compared with the A/N ratio (affected/nonaffected areas) which was adapted from a method proposed by Herholz et al. (*13,16,17*) that has proven to be a robust discriminant for Alzheimer's disease. The A/N ratio was calculated as the averaged CMRglc over the parieto-temporo-frontal association cortex divided by the averaged CMRglc over the sensorimotor and occipital cortex, cerebellum and putamen. The index included both hemispheres simultaneously, not separating each other. For calculation of the ratio in our study, we used regional CMRglc values used in the above analysis for parietal, temporal, frontal, occipital, and sensorimotor cortices. For the cerebellum, we predefined stereotactic grid coordinates (see Appendix) and measured regional CMRglc by the same method applied to the other cortical structures. For the putamen, we averaged pixel values in 1.6 ml of the putamen on a stereotactically standardized PET image set. We compared the A/N ratio with the averaged ΔZ-score over the bilateral parieto-temporo-frontal cortex since the ratio includes both hemispheres (a single representative score for each subject). Sensitivity and specificity to discriminate Alzheimer's disease by the A/N ratio and bilateral ΔZ-score were compared.

Evaluation for ΔZ-score in Cerebrovascular Disease

The ΔZ-score criterion was evaluated in cerebrovascular disease to test specificity and compared to the A/N ratio. Each patient was categorized into false-positive or true-negative for Alzheimer's disease based on the ΔZ-score and the A/N ratio using optimal thresholds determined in the previous section. False-positive and negative cases were examined visually on individuals' surface projection maps.

Data Analysis

The proposed method consists of the following steps: (a) anatomic standardization of an individual's PET image set by stereotactic transformation, (b) data extraction for cortical metabolic activity, (c) data normalization to the thalamic activity, (d) calculation of the Z-score for an individual's data set compared with a normal group (individual-group comparison), (e) calculation of ΔZ-score to contrast metabolic reduction in the association cortex to the sensorimotor cortex, (f) diagnosis based on ΔZ-score and (g) data presentation in three dimensions.

Stereotactic Anatomic Standardization. Stereotactic anatomic standardization is performed by methods described previously (*22–24*). Briefly, an automated algorithm estimates the location of the bicommissural line on a PET mid-sagittal plane and realigns the image set to the standard stereotactic orientation (*22,23*). Regional anatomic differences between the individual's brain on the PET image set and a standard atlas brain are minimized automatically by the linear scaling and nonlinear warping techniques (*24*). Through these steps, an original PET image set is resampled in a standard stereotactic image format, thereby minimizing anatomic variations across subjects while preserving regional metabolic activity.

Data Extraction for Cortical Metabolic Activity. Because data analysis and interpretation concern metabolic abnormalities in the cerebral cortex, the algorithm extracts regional cortical metabolic activity for the subsequent data analyses by a newly developed three-dimensional stereotactic surface projection (3D-SSP) technique. This is an alternative approach to a conventional ROI analysis. The method also treats small anatomic variations of gray-white matter or gray-to-nonbrain borders among subjects

which cannot be removed entirely by the anatomic standardization and enables reliable individual versus group, or group versus group comparisons on a pixel-by-pixel basis. In the standard stereotactic system, pixels located on the outer and medial surface of both hemispheres are predetermined along with three-dimensional vectors perpendicular to the surface at each pixel (see Appendix). For each predetermined surface pixel, the algorithm searches for the highest pixel value in a direction inward along the vector to a six-pixel depth (13.5 mm) into the cortex on an individual's anatomically standardized PET image set and assigns the maximum value to the surface pixel. Surface pixel sets extracted from each individual's PET data are used in the following data analyses.

Data Normalization to Thalamic Metabolic Activity. It is common practice in PET analysis to normalize a data set to a reference region which is known to be less affected in the disease process. In the present work, the algorithm normalizes each pixel value with stereotactic surface coordinates (x, y, z) to the thalamic metabolic activity as follows:

$$\text{Normalized CMRglc}_{(x,y,z)} = \text{CMRglc}_{(x,y,z)}/\text{thalamic CMRglc}. \quad \text{Eq. 1}$$

The thalamic activity is measured by averaging the highest 20 pixels (1.0 cm^2 on medial surface pixels on the surface format) within stereotactic grid coordinates of (a, E, 7–8) plus the anterior half of (a, F, 7–8), independently for each hemisphere (the grid coordinates represent x, y, and z, respectively) (*25*). Because diaschisis from a more severely affected hemisphere could reduce metabolic activity in the ipsilateral thalamus (*26*), the hemisphere containing higher value is used for the normalization. Because of this normalization, the proposed method is applicable to nonquantitative reconstructed image sets.

Normal Reference Database. The mean and s.d. are calculated for each surface pixel using the normalized datasets of 22 normal controls. Because of the limited field of view of the scanner used in this study, superior and inferior structures of the brain were not always included in an image matrix. Therefore, the algorithm counts the effective number of subjects contributing to each pixel and excludes any pixel contributed to by less than four subjects.

Calculation for Individual Z-score Data. A set of surface pixels from a patient with Alzheimer's disease is compared with the normal reference database by means of a Z-score. A Z-score is formed on a pixel-by-pixel basis on the 3D-SSP format as follows:

$$\text{Z-score}_{(x,y,z)} = (N_{MEAN(x,y,z)} - AD_{(x,y,z)})/N_{SD(x,y,z)}, \quad \text{Eq. 2}$$

where $N_{MEAN(x,y,z)}$ and $N_{SD(x,y,z)}$ represent a mean and s.d. of the normal reference data at stereotactic coordinates (x, y, z). $AD_{(x,y,z)}$ represents normalized CMRglc from a patient with Alzheimer's disease at the same pixel coordinates. If either the patient data or normal reference data do not contain sufficient data at a given pixel due to the limited field-of-view, the pixel information is not used in the further analyses. Because of the order of the subtraction, a positive Z-score represents reduced metabolic activity relative to the normal reference data in the following analyses.

Determination of the Primary Sensorimotor Cortex. In the standard stereotactic orientation, there are known variations in location of the primary sensorimotor cortex across subjects (*27,28*). When analyzing an individual's data in the stereotactic system, the method should take these anatomic variations into account. The location of the primary sensorimotor cortex is determined for each hemisphere by an independent search on the Z-score data within 10 pixels (22.5 mm) anteriorly and posteriorly from the standard stereotactic location of the primary sensorimotor cortex using a predefined ROI. A shape of the ROI for the sensorimotor cortex is specified using the standard stereotactic grid coordinates (see Appendix). Since we assume that glucose metabolism in the primary sensorimotor cortex is relatively preserved, the location is determined when mean Z-score averaged across the pixels of the ROI is a minimum.

Diagnostic Index. Since we have hypothesized reduced regional metabolic activity in Alzheimer's disease, an index of Z-score reduction is calculated for cortical areas by averaging pixels only with positive Z-score (pixels with reduced metabolic activity relative to the normal reference database). The indices are calculated independently for each hemisphere in the parietal, temporal, and frontal association cortices, and for the primary sensorimotor and occipital cortices. Pixels located in the parietal, temporal, frontal, and occipital cortices are predetermined using the stereotactic grid coordinates (see Appendix). The location of the primary sensorimotor cortex is searched iteratively by the above technique. Also, indices of Z-score reduction were calculated for the areas averaged over the parieto-temporo-frontal association cortex unilaterally and bilaterally.

To contrast metabolic reduction in the association cortex to the primary sensorimotor cortex, the algorithm calculates ΔZ-score as follows:

$$\Delta\text{Z-score} = [\text{Z-score reduction in the association cortex}] - [\text{Z-score reduction in the primary sensorimotor cortex}]. \quad \text{Eq. 3}$$

A larger Z-score indicates more severe metabolic reduction in the association cortex relative to the primary sensorimotor cortex. When calculating an averaged ΔZ-score over the bilateral parieto-temporo-frontal association cortex, Z-score reductions of the sensorimotor cortex were averaged bilaterally and then subtracted from the bilaterally averaged parieto-temporo-frontal Z-score reduction.

Diagnostic Criteria Based on ΔZ-score. Although there is known asymmetry in the degree of metabolic reduction in the association cortex, bilateral involvement is an important feature of Alzheimer's disease. Isolated unilateral metabolic reduction can be caused by other etiologies, including cerebrovascular disease. In this method, we evaluate each hemisphere independently based on ΔZ-scores, which indicate metabolic abnormalities in the association cortex relative to the primary sensorimotor cortex on the same hemisphere, and then discriminate an Alzheimer's disease pattern when both hemispheres show abnormal ΔZ-scores. Determination of the optimal threshold for ΔZ-score is estimated and evaluated in the following sections.

3D-SSP for Visual Inspection. Since cortical metabolic activity is extracted in a surface format, data can be displayed in the 3D-SSP format (Fig. 1). Individuals' Z-score data, as well as extracted raw data, can be viewed from superior, inferior, right, left, anterior, posterior, and two medial aspects of the brain. A standard contour of the brain is added to the Z-score image to facilitate visual inspection. Stereotactic coordinates can be readily used for more precise localization of signals on those projection views since the entire image processing and presentation are done in the standard stereotactic system.

TABLE 1A
Regional Glucose Metabolism in Normal Subjects and Patients with Alzheimer's Disease (AD): Quantitative CMRglc (mg/100 g/min)

Group		Parietal		Temporal		Frontal		Occipital		Sensorimotor		Thalamus	
		R	L	R	L	R	L	R	L	R	L	R	L
Normal	Mean	7.90	7.77	6.83	6.76	7.88	7.90	8.26	7.97	7.63	7.69	8.78	8.67
(n = 22)	s.d.	1.18	1.10	0.93	0.90	1.14	1.20	1.35	1.29	1.15	1.18	1.48	1.50
	COV(%)[§]	14.9	14.2	13.6	13.4	14.5	15.2	16.4	16.2	15.1	15.3	16.8	17.3
AD	Mean	5.40	5.27	5.19	5.02	6.27	6.10	7.12	7.00	6.80	6.79	7.81	7.75
(n = 37)	s.d.	1.27	1.10	1.00	0.86	1.24	1.23	1.20	1.09	1.04	0.96	1.27	1.14
	COV(%)[§]	23.5	20.8	19.3	17.0	19.8	20.2	16.8	15.6	15.3	14.1	16.3	14.7
	t-test*	−7.51‡	−8.44‡	−6.22‡	−7.39‡	−4.97‡	−5.46‡	−3.35†	−3.10†	−2.82	−3.20†	−2.65	−2.66

*t-test using pooled variances. Negative values indicate reduction in the AD group.
†$p < 0.05$ adjusted for multiple comparisons.
‡$p < 0.01$ adjusted for multiple comparisons.
§COV(%): coefficient of variation, mean/s.d. × 100.

RESULTS

Metabolic Abnormalities in Alzheimer's Disease

Significant glucose metabolic reduction was confirmed quantitatively in most of the cortical structures in Alzheimer's disease (Table 1A). Following data normalization to the thalamic activity, significant relative metabolic reductions in the parietal, temporal, and frontal association cortex were preserved, while no significant relative decreases were detected in the occipital and primary sensorimotor cortex (Table 1B). With normalization, coefficients of variation of regional CMRglc were reduced in all regions in both normal control and Alzheimer's disease.

These regional abnormalities were consistent on the Z-score reduction (Table 2A) and ΔZ-score (Table 2B). Using either scale, significant metabolic reduction ($p < 0.01$) was observed in the parietal, temporal, and frontal association cortex. On ΔZ-score in comparison to Z-score reduction, distinction between normal and Alzheimer's disease became more significant in the parietal and right temporal cortices. The distribution of ΔZ-score values is further demonstrated in Figure 2: the least overlap in the parietal cortex and the largest overlap in the frontal cortex between normal and Alzheimer's disease.

Patterns of Cortical Abnormalities in Alzheimer's Disease

Metabolic abnormalities in the parietal, temporal and frontal association cortices were examined using ΔZ-scores in terms of regional trends and symmetry in metabolic reduction. In Alzheimer's disease, 60 (81%) of 74 hemispheres showed parietal dominance in metabolic reduction (Table 3). Forty-five out of these sixty hemispheres showed second largest reduction in the temporal association cortex. Ten (14%) of 74 hemispheres showed frontal dominance. These patterns of regional metabolic abnormalities differed significantly from those in normal controls.

TABLE 1B
Regional Glucose Metabolism in Normal Subjects and Patients with Alzheimer's Disease (AD): Normalized CMRglc to the Thalamus (%)

Group		Parietal		Temporal		Frontal		Occipital		Sensorimotor	
		R	L	R	L	R	L	R	L	R	L
Normal	Mean	89.9	88.4	77.7	77.1	89.6	89.8	93.7	90.6	86.7	87.5
(n = 22)	s.d.	5.45	5.52	4.43	5.18	5.50	6.03	6.96	7.91	6.01	7.20
	COV(%)[§]	6.06	6.24	5.70	6.73	6.14	6.72	7.42	8.73	6.93	8.23
AD	Mean	68.2	66.6	65.6	63.5	78.8	76.9	90.2	88.6	85.9	85.6
(n = 37)	s.d.	13.1	11.1	9.70	8.37	10.6	11.9	12.5	11.2	8.14	5.77
	COV(%)[§]	19.2	16.7	14.8	13.2	13.5	15.5	13.8	12.7	9.48	6.74
	t-test*	−7.38‡	−8.58‡	−5.52‡	−6.84‡	−4.44‡	−4.74‡	−1.22	−0.738	−0.361	−1.06

*t-test using pooled variances. Negative values indicate reduction in the AD group.
†$p < 0.05$ adjusted for multiple comparisons.
‡$p < 0.01$ adjusted for multiple comparisons.
§COV(%): coefficient of variation, Mean/s.d. × 100.

TABLE 2A
Z-score Reduction in Normal Subjects and Patients with Alzheimer's Disease (AD)

Group		Parietal R	Parietal L	Temporal R	Temporal L	Frontal R	Frontal L	Occipital R	Occipital L	Sensorimotor R	Sensorimotor L
Normal	Mean	0.68	0.66	0.69	0.70	0.66	0.65	0.65	0.64	0.53	0.53
(n = 22)	Max	1.61	1.42	1.52	1.51	1.91	2.18	1.23	1.55	1.61	1.27
	Min	0.20	0.18	0.31	0.23	0.20	0.24	0.13	0.17	0.00	0.00
AD	Mean	3.04	2.91	2.08	2.03	1.73	1.86	1.04	0.93	0.69	0.69
(n = 37)	Max	6.04	5.62	4.88	4.77	4.21	5.39	3.11	2.65	3.08	1.15
	Min	0.60	0.84	0.52	0.71	0.33	0.38	0.00	0.34	0.00	0.20
	U-test*	25‡	10‡	72‡	25‡	140‡	116‡	309	286	307	238

*Mann-Whitney U-test. Smaller values indicate larger reduction in the AD group.
†$p < 0.05$ adjusted for multiple comparisons.
‡$p < 0.01$ adjusted for multiple comparisons.

Twenty-eight (76%) of 37 patients of Alzheimer's disease showed symmetric hemispheric patterns of regional metabolic abnormalities (Table 4). Twenty-four of these 28 patients showed symmetric parietal dominance, and the other four cases showed frontal dominance. A frequency of these symmetrical patterns differed significantly from those in normal controls.

Discrimination of Alzheimer's Disease Using ΔZ-score

True-positive and false-positive fractions for discriminating Alzheimer's disease from normal controls were assessed by changing the ΔZ-score threshold for parietal, temporal and frontal indices, as well as a unilaterally averaged parietal-temporal-frontal index (Fig. 3A). The parietal and unilaterally averaged ΔZ-score showed comparable results, both discriminating better than the temporal and frontal ΔZ-scores. At the false-positive fraction of 0.0 (specificity 100%), the parietal, temporal, frontal, and unilaterally averaged ΔZ-scores showed the best sensitivities of 95%, 81%, 59%, and 97%, respectively. Corresponding ΔZ-score thresholds were 0.55, 0.45, 0.56 and 0.36, respectively.

The same analysis was performed for a bilaterally averaged parietal-temporal-frontal ΔZ-score and A/N ratio (Fig. 3B). For a false-positive fraction of 0.0, the bilaterally averaged ΔZ-score and A/N ratio showed the best sensitivities of 100% and 92%, respectively. Corresponding thresholds were 0.52 and 0.89, respectively. By comparing all the above indices, the parietal ΔZ-score, unilaterally averaged ΔZ-score, bilaterally averaged ΔZ-score and A/N ratio showed comparable results in terms of sensitivity and specificity when discriminating Alzheimer's disease from normal controls.

False-Negative Cases in Alzheimer's Disease

The parietal ΔZ-score resulted in two false-negative cases at the optimal threshold yielding specificity of 100% (Fig. 4, Patients A and B). In both cases, only the left hemisphere was identified as abnormal; thus, the diagnostic criterion of bilateral abnormality was not satisfied. Patients A and B were mildly (CDR = 1) and moderately (CDR = 2) demented, respectively. The unilaterally averaged ΔZ-score resulted in one false-negative (Case A). The bilaterally averaged ΔZ-score showed no false-negatives. The A/N ratio resulted in three false-negatives (Fig. 4, Patients A, C and D). Both Patients C and D were mildly demented (CDR = 1).

TABLE 2B
ΔZ-score in Normal Subjects and Patients with Alzheimer's Disease (AD)

Group		Parietal R	Parietal L	Temporal R	Temporal L	Frontal R	Frontal L	Occipital R	Occipital L
Normal	Mean	0.15	0.13	0.16	0.17	0.13	0.12	0.12	0.11
(n = 22)	Max	0.73	0.55	0.55	0.70	0.57	0.92	0.68	1.03
	Min	−0.15	−0.49	−0.16	−0.44	−0.34	−0.42	−0.65	−0.50
AD	Mean	2.34	2.22	1.39	1.34	1.04	1.17	0.35	0.24
(n = 37)	Max	5.00	4.73	3.47	3.65	3.72	4.25	2.15	1.93
	Min	0.32	0.56	−0.16	0.19	−2.30	−0.44	−1.00	−0.70
	U-test*	6‡	0‡	47‡	37‡	152‡	158‡	340	360

*Mann-Whitney U-test. Smaller values indicate larger reduction in the AD group.
†$p < 0.05$ adjusted for multiple comparisons.
‡$p < 0.01$ adjusted for multiple comparisons.

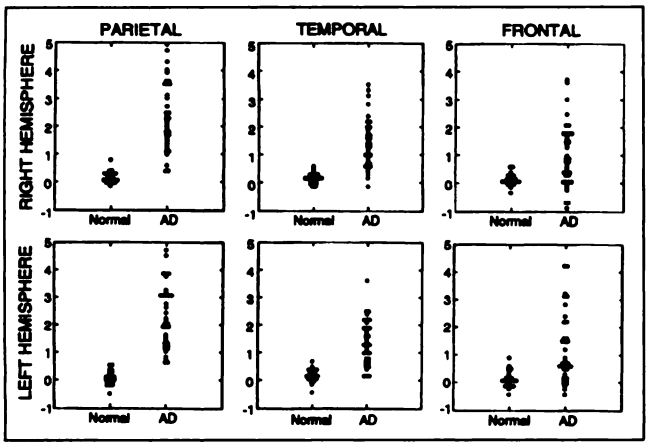

FIGURE 2. ΔZ-score in the parietal, temporal and frontal association cortex in normal subjects and patients with Alzheimer's disease. The vertical axes represent ΔZ-scores. Larger ΔZ-scores indicate more severe metabolic reduction in the above regions in comparison with that in the primary sensorimotor cortex.

False-Positive Cases in Cerebrovascular Disease

The parietal ΔZ-score and unilaterally averaged ΔZ-score showed no false-positives in the group of cerebrovascular disease patients. However, the parietal ΔZ-score indicated hemispheric abnormality (not bilateral, therefore not diagnostic) in one multi-infarct patient (Fig. 5, patient E), while the unilaterally averaged ΔZ-score indicated hemispheric abnormality in two multi-infarct patients (Fig. 5, Patients E and F) and one patient with MCA infarction (Patient G). The bilaterally averaged ΔZ-score yielded one false-positive in a multi-infarct patient (Patient E). The A/N ratio resulted in three false-positives; two multi-infarct patients (Patients E and F) and one patient with MCA infarction (Patient G). Although some of the quantitative indices used for analysis yielded false-positives in certain cases, distributions of metabolic abnormalities were clearly distinguishable from those of Alzheimer's disease by visual inspection.

TABLE 3
Regional Trends in Cortical Metabolic Reduction* in Alzheimer's Disease (AD) and Normal Groups

	AD (n = 74)	Normal (n = 44)
P > T > F†	45	12
P > F > T	15	0
F > P > T	8	5
T > P > F	3	13
F > T > P	2	6
T > F > P	1	8

*The ranking is based on ΔZ-scores. †P, T, and F represent the parietal, temporal and frontal association cortices, respectively. Each hemisphere was analyzed independently. Group difference: $p < 0.0001$ (chi-square test).

TABLE 4
Hemispheric Asymmetry in Cortical Metabolic Reduction* in Alzheimer's Disease

Symmetrical (n = 28)			Asymmetrical (n = 9)		
RT	LT	n	RT	LT	n
P > T > F –	P > T > F†	19	P > T > F –	T > P > F	3
P > F > T –	P > F > T	5	P > F > T –	F > P > T	2
F > P > T –	F > P > T	3	P > F > T –	P > T > F	2
F > T > P –	F > T > P	1	P > T > F –	P > F > T	1
			P > T > F –	T > F > P	1

*The ranking is based on ΔZ-scores. †P, T and F represent the parietal, temporal and frontal association cortices, respectively. In the normal group, hemispheric symmetry and asymmetry were observed in 10 and 12 cases, respectively.
Group difference: $p < 0.05$ (chi-square test).

DISCUSSION

Patterns of cortical metabolic abnormalities in Alzheimer's disease were examined using a newly developed method of cortical data extraction and a ΔZ-score based on individual versus normal database comparison. Using ΔZ-scores, the proposed method enables objective and accurate discrimination of probable Alzheimer's disease. Three-dimensional stereotactic surface projections, transformed from the set of extracted cortical data, facilitated visual localization of functional signals. These results indicate significant advantages of the proposed method for interpretation of functional brain PET images.

In the proposed method, recognition of an Alzheimer's disease pattern is based on independent assessment of hemispheric abnormalities in the association cortex in comparison to those in the primary sensorimotor cortex, and is distinct from previous approaches. Although asymmetry in the degree of metabolic reduction can exist (*4,9,10,15,18–20*), both hemispheres are generally involved in Alzheimer's disease, making comparison of homologus regions in both hemispheres less sensitive to detect symmetric abnormalities. Diagnosis based on independent hemispheric assessment of

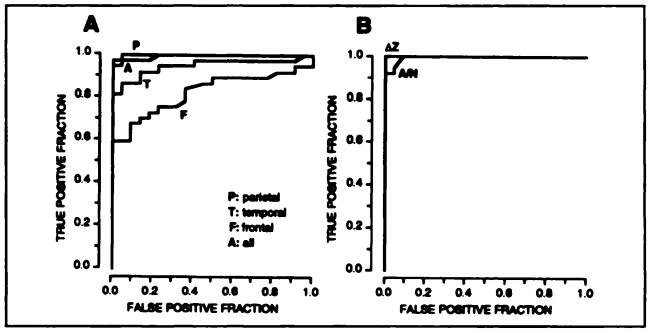

FIGURE 3. Sensitivity and specificity of ΔZ-score discrimination for Alzheimer's disease. (A) Comparison of ΔZ-scores for parietal, temporal, frontal and unilaterally averaged parietal-temporal-frontal association cortex. (B) Comparison between bilaterally averaged parietal-temporal-frontal ΔZ-score and A/N ratio.

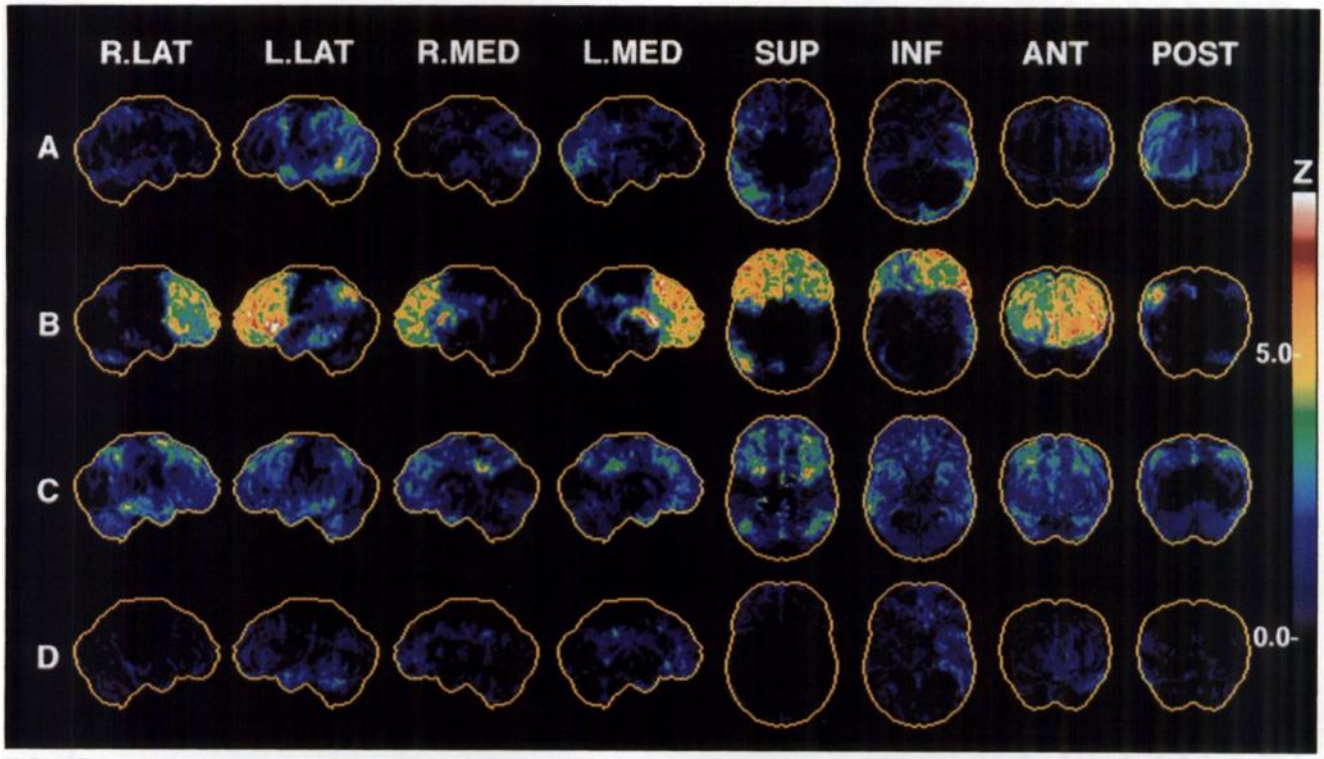

FIGURE 4. False-negatives in Alzheimer's disease based on ΔZ-score and A/N discrimination. 3D-SSP Z-score views (only demonstrating areas of metabolic reduction). Patient A (mildly demented) shows significant metabolic abnormalities in the left hemisphere only. Patient B (moderately demented) shows frontal dominance in metabolic reduction with additional decrease only in the left parietal-temporal association cortex. Patient C (mildly demented) shows metabolic reduction in the frontal-parietal-temporal association cortex bilaterally with mild reduction in the cerebellum. Patient D (mildly demented) shows minimal left temporal-frontal reduction. Patient A has a false-negative based on the parietal ΔZ-score, unilaterally averaged parietal-temporal-frontal ΔZ-score, and A/N ratio. Patient B has a false-negative based on the parietal ΔZ-score. Patients C and D have false-negatives based on the A/N ratio.

metabolic reduction not only showed good sensitivity but also high specificity. When including both hemispheres together, without separation, using a ΔZ-score or A/N ratio, sensitivity became slightly higher, but specificity dropped due to false-positive cases in patients with single or multiple infarctions, which could be problematic when differentiating ischemic dementia from Alzheimer's disease in a clinical setting. Since the proposed method is constructed according to a priori knowledge of metabolic abnormalities in Alzheimer's disease, the approach is also distinct from methods relying on neuronal networks or functions generated by a computer (*37*). Incorporation of new additional knowledge about metabolic features in Alzheimer's disease (an optimal reference region for data normalization, diagnostic criteria based on other regional abnormalities, etc.) might even improve accuracy in discrimination, which is open for further investigations.

Analysis of patterns of regional metabolic reduction showed either asymmetry or frontal-temporal dominance in certain cases. For example, ten hemispheres showed frontal-dominant reduction (symmetrical in four cases). Some of these cases demonstrated prominent metabolic reduction in the frontal lobe, which is not the typical parieto-temporal reduction indicative for Alzheimer's disease by visual inspection. Based on quantitative analysis of ΔZ-score with a predetermined threshold, however, the parietal association cortex is also involved bilaterally in most of those cases, permitting reliable distinction of probable Alzheimer's disease using the parietal cortex as a discriminator. This indicates a complementary role of the diagnostic index with visual inspection. The ΔZ-score is derived from Z-score reduction calculated between an individual's dataset and a normal database. Individual-to-group comparisons enable image analysis to focus on only areas with metabolic reduction, partly resulting in such high sensitivity of the proposed method. In fact, three cases of questionably demented patients (CDR = 0.5 at the time of PET imaging) were distinguished from normal subjects correctly. This preliminary result emphasizes the use of glucose metabolic PET studies as a part of the clinical diagnostic examinations in patients suspected of Alzheimer's disease. The ΔZ-score criteria in the proposed method, however, was optimized based on the NINCDS-ADRDA clinical diagnosis for probable Alzheimer's disease. Even though the method can distinguish a cerebral glucose metabolic pattern of probable Alzheimer's disease accurately, it might not differentiate definite Alzheimer's disease from other dementing neurodegenerative disorders which might cause a similar pattern of cerebral metabolic abnormalities. Further investigations incorporating postmortem pathological examinations are necessary to address the ability of glucose metabolic PET studies to differentiate such related dementing disorders.

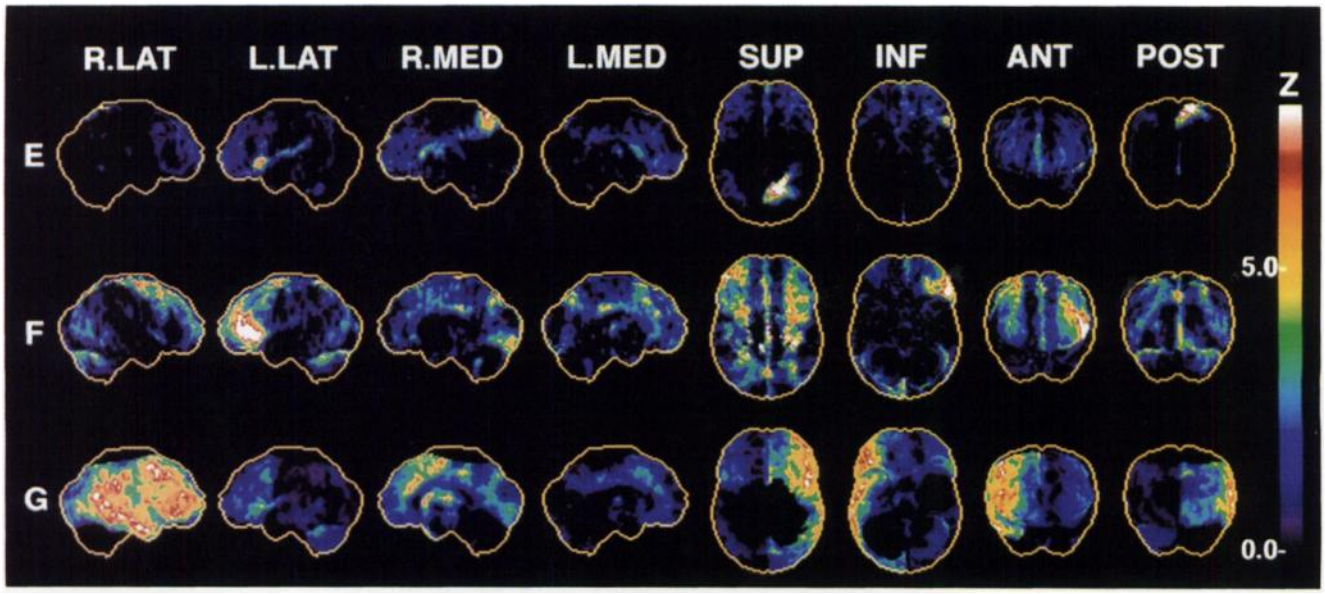

FIGURE 5. False-positives in cerebrovascular disease based on ΔZ-score and A/N ratio discrimination for Alzheimer's disease. Three-dimensional-SSP Z-score views demonstrate areas of metabolic reduction. Patient E has at least two areas of metabolic reduction in the right superior parietal cortex and left frontal operculum. Patient F shows metabolic reduction in the frontal and parietal cortex bilaterally associated with severe focal decrease in the left frontal cortex and mild-to-moderate decrease in the occipital cortex and cerebellum. Patient G shows a large area of metabolic reduction, corresponding to the right middle cerebral artery territory, associated with mild decrease in the left frontal cortex and cerebellum. Patient E has a false-positive based on the bilaterally averaged parietal-temporal-frontal ΔZ-score and A/N ratio. Patients F and G have false-positives based on the A/N ratio.

A method for extracting cortical metabolic activity in a PET image set onto representative stereotactic surface pixels is an alternative approach to conventional ROI analysis, preserving both metabolic and spatial information of PET. This method is an effective means of data reduction for a PET brain image set. When compared to ROI analysis, which reduces metabolic information of the brain (typically more than one-hundred thousand pixels) to a few hundred regions with only gross anatomic information, the proposed cortical surface extraction method reduces the same amount of data to approximately sixteen thousand pixels (80%–90% reduction) while preserving stereotactic pixel coordinates. There is an obvious tradeoff between data reduction and preservation of spatial information. A pixel-by-pixel statistical analysis with less intensive adjustment for multiple comparison can be performed on this reduced data format. Since the algorithm searches cortical location in the direction of the surface vector at each pixel, small displacements of the gray matter between the standard stereotactic coordinates and individual's brain can be compensated by this method. This feature is important when comparing PET datasets of different groups on a pixel-by-pixel basis because anatomic standardization can minimize, but not remove entirely, individuals' anatomic variations (*24*). Without such considerations, pixel-based inter-group comparisons not only reveal regional metabolic differences, but also are confounded with anatomic mismatches. Although the extracted cortical data in the current algorithm are the highest pixels along each surface vector, demonstrating reliable discrimination for Alzheimer's disease, it needs to be investigated further whether the single highest pixel or an average of the few highest pixels would be a more reliable representation for cortical activity, especially in terms of quantitative accuracy. A limitation of this approach is that the structures located deep within the brain, such as the lenticular nucleus and insula, cannot be expressed in this format, although combination with ROI analysis for such anatomically distinct structures can obviate this problem.

In the proposed method, surface pixel data are normalized to the thalamic activity prior to the analysis. Data normalization can remove systemic errors inherent in quantitative measurements (accuracy in input function, cross-calibration, etc.), minimize global baseline differences of cerebral metabolic activity across subjects, and enhance regional metabolic reduction in contrast to normal reference areas, all of which increase sensitivity of detection of regional abnormalities. In fact, regional metabolic profiles in the current study showed smaller coefficients of variance and higher levels of significance for metabolic reduction in the parietal-temporal association cortex following normalization (Table 1B). Furthermore, data normalization enables applications of the proposed technique to nonquantitative PET and SPECT data sets. The literature and our prior observations both show that the use of the thalamus or primary cortex is more suitable for normalization than global or cerebellar activity (*38,39*). Since cortical metabolic abnormalities on PET are the diagnostic features for Alzheimer's disease, we have used a subcortical structure, the thalamus, for normalization in the current study. The thalamus also has a distinct shape and is located just above the intercommissural line, the standard line defining the stereotactic coordinate system, thereby ensuring reliable and accurate localization. In certain cases of Alzhei-

mer's disease (*26*), as well as in stroke (*40*), there is metabolic reduction in the thalamus due to remote effects from ipsilateral hemispheric abnormalities. Thus, we have chosen to use the higher value from either hemisphere for normalization, thereby minimizing bias caused by such remote effects.

In addition to quantitative analysis, a cortical extraction dataset is suitable for visual inspection of a PET image set. Since regional cortical metabolic activity is assigned to representative surface pixels, the data set can be viewed readily in 3D-SSP views. As shown in the figures, any data set in a surface format, such as cortical extraction data and parametric Z-score data, can be presented as the 3D-SSP views. Because of the cortical extraction procedure in three dimensions, the proposed stereotactic surface projection technique differs from simple two-dimensional projection views and does not introduce biases or artifacts at brain edges. Any additional views, such as oblique or rotating views, can be prepared easily from a cortical extraction data set. This greatly facilitates visual inspection of functional brain image sets. Since certain stroke cases, e.g., infarction in the unilateral parietal and contralateral temporal association cortices, incidentally could result in abnormal ΔZ-scores, visual inspections for distribution of metabolic reduction in the brain are necessary when evaluating metabolic patterns of Alzheimer's disease. As demonstrated in Figures 1, 4 and 5, 3D-SSP provides omnibus and comprehensive views of metabolic abnormalities in the entire cortex, enabling reliable and consistent visual inspection. Diagnostic values of visual interpretation using 3D-SSP are currently under investigation based on inspections by multiple observers (*41*). With a simple user-interactive image analysis program, one can localize functional signals more precisely on 3D-SSP by referring to stereotactic coordinates. Conventional ROI analyses also can be performed on these views for further quantitative assessment. On currently available workstations, computation time required for the proposed method is acceptable for a routine use. Anatomic standardization takes approximately 40 min on a SparcStation 10 workstation (Sun Microsystems, Mountain View, CA), and subsequent surface data extraction, comparison, and presentation take less than 5 min. Therefore, 3D-SSP can be used as a 'brain map' in clinical settings, similar to cardiac polar maps (*42,43*) and SPECT perfusion maps (*44*) but with accurate signal localization and quantification capabilities.

CONCLUSION

We have presented a new diagnostic approach in Alzheimer's disease using the three-dimensional stereotactic surface projection technique. The 3D-SSP and the normal reference database of FDG-PET enable quantitative data extraction, subsequent statistical data analysis, comprehensive data display in three dimensions and accurate localization for metabolic abnormalities in the stereotactic coordinate system. Diagnostic indices based on the database comparison provided accurate discrimination for patients with probable Alzheimer's disease. The proposed method promises to be a useful approach for quantitative as well as objective visual interpretations of functional brain images. A further study is currently being undertaken to confirm accuracy of the method in prospectively collected patient population.

ACKNOWLEDGMENTS

This study was supported in part by grants RO1-NS24896 from the National Institutes of Health and DE-FG02-87-ER60561 from the Department of Energy.

APPENDIX

Determination of Stereotactic Surface Pixels of the Brain

Pixels located on the outer and medial surface of the brain are predetermined using a MRI set. [^{18}F]FDG and T1-weighted MRI sets were obtained from a 53-yr-old man with no structural abnormalities in the brain confirmed by radiologists and aligned in the same orientation using an user-interactive program based on the work of Pietrzyk et al. (*45*). Anatomic standardization techniques (*22–24*) were applied to the [^{18}F]FDG image set, creating transformation parameters. Then the co-registered MRI set was transformed to the standard stereotactic atlas coordinates using those parameters. Structures such as the scalp and bone marrow on the MRI set were removed by applying a threshold suitable for delineating cortical margins on the co-registered [^{18}F]FDG image set. Residual extra-cerebral pixels on the MRI set were removed manually. The right hemisphere of the brain was removed, and the left hemisphere was transposed to the right side, creating a symmetrical brain. Then the MRI set was transformed to a binary image set by assigning one to pixels with intensity higher than that of cerebrospinal fluid and zero to the rest of the pixels. By viewing this binary image set of the brain in three dimensions from superior, inferior, right, left, anterior, posterior and medial aspects, pixels located on the outer and inner surface of the brain were determined. At each surface pixel, a center-of-mass (with each pixel weighted by 1 or 0) within a sphere with four-pixel (9 mm) radius (the center of the sphere corresponds to the surface pixel) was calculated on the binary image set. A vector from the surface pixel to the center-of-mass was used to approximate the perpendicular to the brain surface. More than 16,000 surface pixels (and corresponding vectors) covering the outer and inner surface of both hemispheres were predetermined in stereotactic coordinates.

Stereotactic Grid Coordinates for Cortical Areas

Stereotactic grid coordinates are used for averaging regional metabolic activity for the following structures on the surface format (*25*). These specifications do not necessarily encompass the entire areas of the given structure. For example, the frontal and sensorimotor coordinates used in the current study do not include medial aspects. The occipital coordinates include mainly the primary visual cortex. The cerebellar coordinates do not include the superior portion of the cerebellum due to unreliable separation from the fusiform gyrus and inferior occipital cortex.

Sensorimotor cortex:
(c–d, E1, 3–7), (b, E2, 1–2), (c–d, E2, 1–4), (b–d, E3, 1–2)
Parietal association cortex:
(a–d, G, 1–5), (a–d, H, 1–4)
Temporal association cortex:
(c–d, D, 10–12), (c–d, E, 9–12), (c–d, F, 7–10), (c–d, G, 6–10)

Frontal association cortex:
(b–d, A, 3–11), (b–d, B, 2–11), (b–d, C, 1–11), (b–d, D, 1–4)
Occipital cortex:
(a, H–I, 6–9)
Cerebellum:
(a–d, G–H, 11–13*), (a–d, I, 12)

*The grid z-coordinate '13' does not exist in the original definition. We define the grid 13 as the grid inferior to the grid 12 with the same spacing and thickness as the grid 12.

REFERENCES

1. Farkas T, Ferris SH, Wolf AP, et al. ^{18}F-2-deoxy-2-fluoro-D-glucose as a tracer in the positron emission tomographic study of senile dementia. *Am J Psychiatry* 1982;139:352–353.
2. Benson DF, Kuhl DE, Hawkins RA, Phelps ME, Cummings JL, Tsai SY. The fluorodeoxyglucose ^{18}F scan in Alzheimer's disease and multi-infarct dementia. *Arch Neurol* 1983;40:711–714.
3. Friedland RP, Budinger TF, Ganz E, et al. Regional cerebral metabolic alterations in dementia of the Alzheimer type: PET with [^{18}F]fluorodeoxyglucose. *J Comput Assist Tomogr* 1983;7:590–598.
4. Foster NL, Chase TN, Fedio P, Patronas NJ, Brooks RA, Di Chiro G. Alzheimer's disease: focal cortical changes shown by positron emission tomography. *Neurology* 1983;33:961–965.
5. Kuhl DE. Imaging local brain function with emission computed tomography. *Radiology* 1984;150:625–631.
6. Foster NL, Chase TN, Mansi L, Brooks R, Fedio P, Patronas NJ, Di Chiro G. Cortical abnormalities in Alzheimer's disease. *Ann Neurol* 1984;16:649–654.
7. Kuhl DE, Metter EJ, Riege WH. Patterns of cerebral glucose utilization in depression, multiple infarct dementia, and Alzheimer's disease. *Res Pub Assoc Res Nerv Ment Dis* 1985;63:211–226.
8. Cutler NR, Haxby JV, Duara R, et al. Clinical history, brain metabolism, and neuropsychological function in Alzheimer's disease. *Ann Neurol* 1985;18: 298–309.
9. Friedland RP, Budinger TF, Koss E, Ober BA. Alzheimer's disease: anterior-posterior and lateral hemispheric alterations in cortical glucose utilization. *Neurosci Lett* 1985;53:235–240.
10. Duara R, Grady C, Haxby J, et al. PET in Alzheimer's disease. *Neurology* 1986;36:879–887.
11. McGeer PL, Kamo H, Harrop R, et al. Positron emission tomography in patients with clinically diagnosed Alzheimer's disease. *Can Med Assoc J* 1986;134:597–607.
12. Polinsky RJ, Noble H, Di Chiro G, Nee LE, Feldman RG, Brown RT. Dominantly inherited Alzheimer's disease: cerebral glucose metabolism. *J Neurol Neurosurg Psychiatry* 1987;50:752–757.
13. Heiss WD, Szelies B, Kessler J, Herholz K. Abnormalities of energy metabolism in Alzheimer's disease studies with PET. *Ann N Y Acad Sci* 1991;640:65–71.
14. Guze BH, Hoffman JM, Baxter LR Jr, Mazziotta JC, Phelps ME. Functional brain imaging and Alzheimer-type dementia. *Alzheimer Dis Assoc Disord* 1991;5:215–230.
15. Nyback H, Nyman H, Blomqvist G, Sjorgren I, Stone-Elander S. Brain metabolism in Alzheimer's dementia: studies of ^{11}C-deoxyglucose accumulation, CSF monoamine metabolites and neuropsychological test performance in patients and healthy subjects. *J Neurol Neurosurg Psychiatry* 1991;54:672–678.
16. Mielke R, Herholz K, Grond M, Kessler J, Heiss WD. Differences of regional cerebral glucose metabolism between presenile and senile dementia of Alzheimer type. *Neurobiol Aging* 1992;13:93–98.
17. Herholz K, Adams R, Kessler J, Szelies B, Grond M, Heiss WD. Criteria for the diagnosis of Alzheimer's disease with PET. *Dementia* 1990;1:156–164.
18. Cutler NR, Duara R, Creasey H, Grady CL, Haxby JV, Schapiro MB, Rapoport SI. NIH Conference. Brain imaging: aging and dementia. *Ann Intern Med* 1984;101:355–369.
19. Koss E, Friedland RP, Ober BA, Jagust WJ. Differences in lateral hemispheric asymmetries of glucose utilization between early- and late-onset Alzheimer-type dementia. *Am J Psychiatry* 1985;142:638–640.
20. McGeer EG, Peppard RP, McGeer PL, et al. Fluorine-18-fluorodeoxyglucose positron emission tomography studies in presumed Alzheimer cases, including 13 serial scans. *Can J Neurol Sci* 1990;17:1–11.
21. Kumar A, Schapiro MB, Haxby JV, Grady CL, Friedland RP. Cerebral metabolic and cognitive studies in dementia with frontal lobe behavioral features. *J Psychiatr Res* 1990;24:97–109.
22. Minoshima S, Berger KL, Lee KS, Mintun MA. An automated method for rotational correction and centering of three-dimensional functional brain images. *J Nucl Med* 1992;33:1579–1585.
23. Minoshima S, Koeppe RA, Mintun MA, Berger KL, Taylor SF, Frey KA, Kuhl DE. Automated detection of the intercommissural (AC-PC) line for stereotactic localization of functional brain images. *J Nucl Med* 1993;34: 322–329.
24. Minoshima S, Koeppe RA, Frey KA, Kuhl DE. Anatomical standardization: linear scaling and nonlinear warping of functional brain images. *J Nucl Med* 1994;35:1528–1537.
25. Talairach J, Tournoux P. *Co-planar stereotaxic atlas of the human brain.* Stuttgart, New York: Thieme, 1988.
26. Akiyama H, Harrop R, McGeer PL, Peppard R, McGeer EG. Crossed cerebellar diaschisis and uncrossed basal ganglia and thalamic diaschisis in Alzheimer's disease. *Neurology* 1989;39:541–548.
27. Talairach J, Szikla G, Tournoux P, et al. *Atlas d'anatomie stéréotaxique du télencéphale*, Paris: Masson & C^{ie}, 1967.
28. Steinmetz H, Fürst G, Freund HJ. Cerebral cortical localization: application and validation of the proportional grid system in MRI. *J Comput Assist Tomogr* 1989;13:10–19.
29. McKhann G, Drachman D, Folstein M, Katzman R, Price D, Stadlan EM. Clinical diagnosis of Alzheimer's disease: report of the NINCDS-ADRDA work group under the auspices of department of health and human services task force on Alzheimer's disease. *Neurology* 1984;34:939–944.
30. Tierney MC, Fisher RH, Lewis AJ, Zorzitto ML, Snow WG, Reid DW, Nieuwstraten P. The NINCDS-ADRDA work group criteria for the clinical diagnosis of probable Alzheimer's disease: a clinicopathologic study of 57 cases. *Neurology* 1988;38:359–364.
31. Hachinski VC, Iliff LD, Zilhka E, et al. Cerebral blood flow in dementia. *Arch Neurol* 1975;32:632–637.
32. Wade J, Hachinski V. Revised ischemic score for diagnosing multi-infarct dementia. *J Clin Psychiatry* 1986;47:437–438.
33. Hughes CP, Berg L, Danziger WL, Coben LA, Martin RL. A new clinical scale for the staging of dementia. *Brit J Psychiat* 1982;140:566–572.
34. Hutchins GD, Holden JE, Koeppe RA, Halama JR, Gatley SJ, Nickles RJ. Alternative approach to single-scan estimation of cerebral glucose metabolic rate using glucose analogs, with particular application to ischemia. *J Cereb Blood Flow Metab* 1984;4:35–40.
35. Efron B. *The jackknife, the bootstrap, and other resampling plans.* Philadelphia: Society for Industrial and Applied Mathematics; 1982;38:5–6.
36. Metz CE. Basic principles of ROC analysis. *Semin Nucl Med* 1978;8:283–298.
37. Kippenhan JS, Barker WW, Nagel J, Grady C, Duara R. Neural-network classification of normal and Alzheimer's disease subjects using high- and low-resolution PET cameras. *J Nucl Med* 1994;35:7–15.
38. Kushner M, Tobin M, Alavi A, et al. Cerebellar glucose consumption in normal and pathologic states using fluorine-FDG and PET. *J Nucl Med* 1987;28:1667–1670.
39. Syed GM, Eagger S, Toone BK, Levy R, Barrett JJ. Quantification of regional cerebral blood flow (rCBF) using ^{99m}Tc-HMPAO and SPECT: choice of the reference region. *Nucl Med Commun* 1992;13:811–816.
40. Kuhl DE, Phelps ME, Kowell AP, Metter EJ, Selin C, Winter J. Effects of stroke on local cerebral metabolism and perfusion: mapping by emission computed tomography of ^{18}FDG and $^{13}NH_3$. *Ann Neurol* 1980;8:47–60.
41. Burdette JH, Minoshima S, Tran DD, Kuhl DE. Improved diagnostic performance with 3D stereotaxic surface projections of functional brain images: clinical application in Alzheimer's disease. *Radiology* 1994;193(P):163.
42. Eisner R, Churchwell A, Noever T, et al. Quantitative analysis of the tomographic ^{201}Tl myocardial bullseye display: critical role for correcting for patient motion. *J Nucl Med* 1988;29:91–97.
43. Johnson TK, Kirch DL, Hasegawa BH, Sklar J, Hendee WR, Steele PP. Early description of "bull's-eye" plot for emission cardiac tomography. *J Nucl Med* 1988;29:267–268.
44. Lamoureux G, Dupont RM, Ashburn WL, Halpern SE. "CORT-EX:" a program for quantitative analysis of brain SPECT data. *J Nucl Med* 1990; 31:1862–1871.
45. Pietrzyk U, Herholz K, Heiss WE. Three-dimensional alignment of functional and morphological tomograms. *J Comput Assist Tomogr* 1990;14:51–59.